Available online at www.sciencedirect.com
ScienceDirect
Journal of Power Sources 158 (2006) 874–878
JOURNAL OF POWER SOURCES
www.elsevier.com/locate/jpowsour

Short communication

Battery condition monitoring (BCM) technologies about lead–acid batteries

Tetsuro Okoshi [a,*], Keizo Yamada [a], Tokiyoshi Hirasawa [a], Akihiko Emori [b]

[a] *Advanced Battery Development Center, Shin-Kobe Electric Machinery Company Limited, Saitama 369-0297, Japan*
[b] *Hitachi Research Laboratory, Hitachi Limited, Hitachi-Shi, Ibaraki 319-1292, Japan*

Available online 6 January 2006

Abstract

A novel battery condition monitoring (BCM) technology for lead–acid batteries has been developed. We have developed a highly reliable SOC monitor that improves the estimated precision of the stored capacity to ±5% for both the flooded type and VRLA. A novel SOC estimation algorithm was also developed. The SOC value was obtained by the weighting combination of the values from the SOC–DCR table and the current integration. Kalman Filtering Theory contributed to developing this system. In order to improve the accuracy of the SOC–DCR table, we have derived a theoretical equation for the SOC–DCR relationship. This equation helps to interpolate the data and improve the accuracy of the SOC–DCR table.

Keywords: Battery condition monitoring; Lead–acid batteries; VRLA; State of charge (SOC); Direct current resistance (DCR); State of health (SOH)

1. Introduction

On the basis of the globally increasing interests regarding environmental problems such as air pollution, acid rain, the greenhouse effect and so on, automakers have been developing next generation automotive systems to reduce CO_2 and NOx [1,2]. Fig. 1 is a roadmap of the next generation automotive system and batteries. It is predicted that the X-By-Wire, idling stop system (ISS) and 42 V system (Mild hybrid system) will spread around the world. In these new systems, electric power has replaced hydraulics. Lead–acid batteries will be selected for the 12–36 V region because of their low cost and easy use. In these systems, as the load on the batteries increases, the life shortens. Electric power is supplied from the batteries for braking and steering, so if a battery has problems, the system will be seriously affected. So we always need to monitor the state of the batteries, such as SOC and SOH, and a more reliable SOC monitor of automotive lead–acid batteries is required.

2. Experimental

2.1. Test cells

VRLA and flooded type of lead–acid batteries are used in this study.

2.1.1. VRLA type

Capacity is 19 Ah, voltage is 36 V and weight is 27 kg. This battery is developed for the 42 V system.

2.1.2. Flooded type

Capacity is 100 Ah, voltage is 12 V and weight is 20 kg. This battery is used for the 14 V truck or bus system and is now commercially available.

2.2. Measurement of SOC–DCR relationship

This procedure is carried out at 25 °C. The SOC is adjusted to various levels in the range from 0 to 100% by discharging at the 0.2 C rate from 100% SOC, which is the fully charged state. After the SOC is adjusted, the batteries are left for 12 h, because about 12 h is needed to reduce the polarization. At the various SOCs, the DCR is measured by discharging a 500 A current in one second. The voltage drop is measured by using a data logger and DCR is determined.

2.3. SOH change method

The SOH is also changed in the new SOC–DCR procedure. As mentioned later, the SOH is defined as the degree of decrease of the nominal capacity. The degree of decrease is determined by a charge/discharge pattern cycle. The charge condition is 14 V, 25 A over 10 min and the discharge is 25 A over 4 min. This charge/discharge pattern cycle is carried out at 40 °C.

* Corresponding author.
E-mail address: t.okoshi@shinkobe-denki.co.jp (T. Okoshi).

0378-7753/$ – see front matter © 2005 Elsevier B.V. All rights reserved.
doi:10.1016/j.jpowsour.2005.11.008

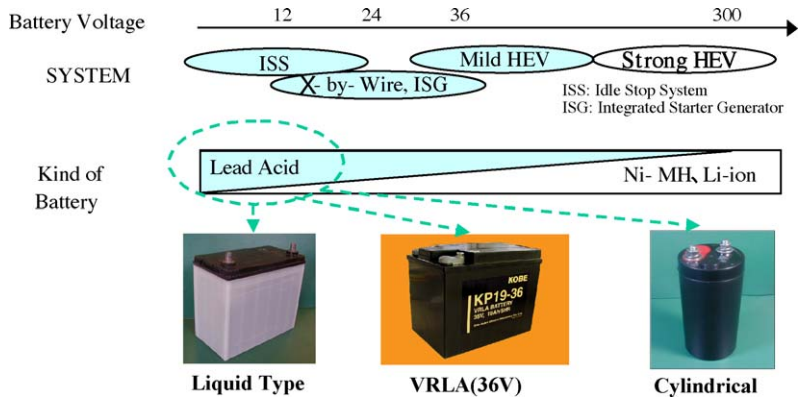

Fig. 1. Road map of next automotive systems and batteries in near future.

3. Results and discussion

3.1. Definition of the state of lead–acid batteries

SOC and SOH are popular parameters for representing the state of lead–acid batteries. SOC is an abbreviation for the "State Of Charge" and is a measure of the deliverable capacity of the battery with respect to its nominal capacity. The nominal capacity is determined at a specified temperature on a new fully charged battery. The SOH is the abbreviation for the "State Of Health" and is the nominal capacity of the initial time to the present time, represented by Eq. (1).

$$\text{SOH} = \frac{(\text{Nominal capacity at present time})}{(\text{Nominal capacity at initial})} \quad (1)$$

The definitions of SOC and SOH are now being discussed by the MIT consortium, but now there is no formal equation. In this study these capacities are measured at 0.2 C [3].

3.2. Relationship between SOC and DCR of lead–acid batteries

The selection of a highly sensitive parameter is very important for the accurate monitoring of the SOC and SOH. According to previous studies, the internal resistance is the optimum parameter for estimating the SOC and SOH. There are two ways of measuring the internal resistance, that is, direct current resistance (DCR) and alternating current resistance (ACR) [4–6]. There are many result of monitoring the SOC and SOH using ACR, but measurement response of the ACR is very slow, so it is not appropriate for automotive systems, because a quick response is required. The DCR is more convenient, because it can be easily measured by the current and voltage. Fig. 2 shows the charge and discharge characteristics of a battery in the ISS mode. Three to four hundred amperes of current occur during cranking. The cycle of running, idling stop and restart is repeated. DCR is defined by Eq. (2) as follows, i.e. change ratio of voltage to current during cranking.

$$\text{DCR} = \frac{\Delta V}{\text{VI}} \quad (2)$$

Fig. 3 shows the relationship between the DCR and SOC of a VRLA. Temperature: 25 °C, Test sample: 19 Ah, 2 V single cell of 36 V VRLA.

Fig. 4 shows the relationship between the DCR and SOC of the flooded type. Temperature: 25 °C, Test sample: 52 Ah, 12 V cell. In this case, the SOC is represented as an absolute value "Ah".

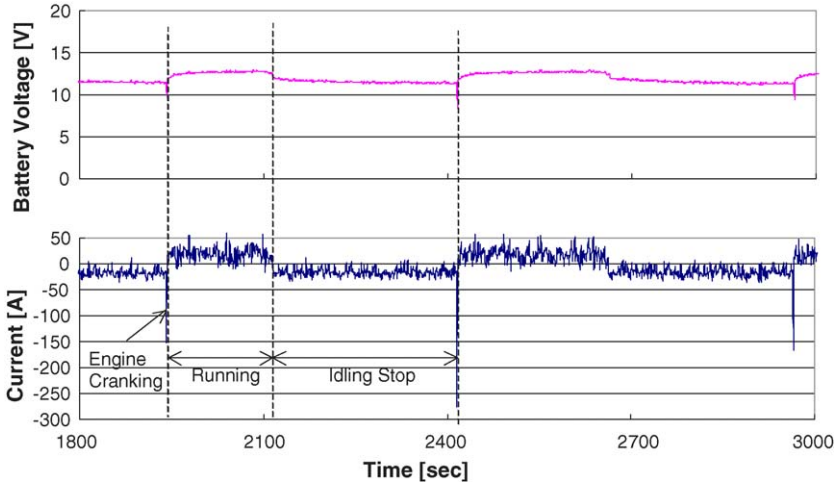

Fig. 2. Charge and discharge characteristics of a battery at ISS mode.

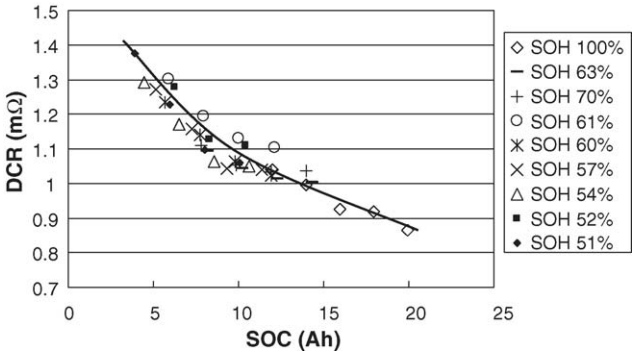

Fig. 3. Relationship between DCR and SOC of VRLA. Temperature: 25 °C; Ampere: 500 A, 1 s; Test sample: VRLA 2 V, 20 Ah (0.2 C).

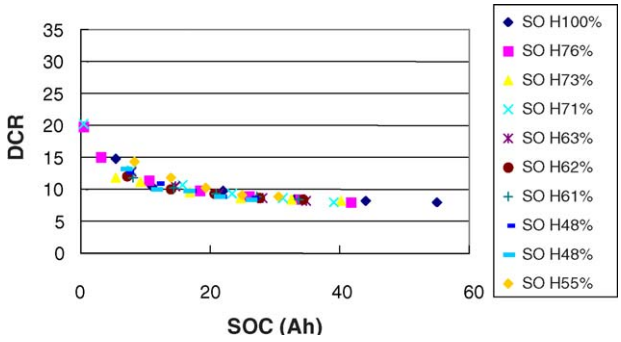

Fig. 4. Relationship between DCR and SOC of flooded type. Temperature: 25 °C; Ampere: 500 A, 1 s; Test sample: liquid type 12 V, 52 Ah (0.2 C).

The following facts were clarified by these results:

(1) SOC and DCR do not have a linear relationship.
(2) Considering the SOH, the DCR plot is slightly scattered versus the SOC, but the DCR is on the curve line to the SOC.
(3) As shown in Fig. 3, for the VRLA, the SOC–DCR table is very sensitive to the low SOC level below 10 Ah (SOC (%) = 50%). However, for the high SOC level, the change ratio of the DCR is low.
(4) As shown in Fig. 4, for the flooded type, the SOC–DCR table is very sensitive to the low SOC level below 10 Ah (SOC (%) = 20%). However, for the high SOC level, the change ratio of the DCR is low and the relationship is almost flat.

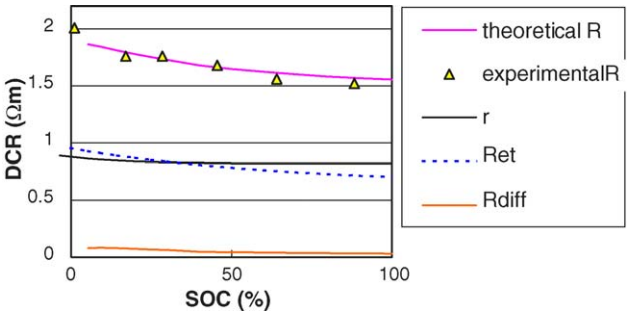

Fig. 6. Comparison between calculated values from the theoretical equation and measured values.

3.3. Theoretical equation of relationship between SOC and DCR of lead–acid batteries

We concluded that we are able to monitor the SOC by accurately using the SOC–DCR table. By the way, there is a problem that we have to obtain much data in order to measure the SOC, because there are many parameters like temperature, SOC and cell size. If we get a theoretical equation for the relationship between the SOC and DCR, it will be very useful for developing BCM technology.

We tried to solve the SOC–DCR characteristics of lead–acid batteries. Fig. 5 shows the reaction process on the surface of the electrode of a lead–acid battery during discharge. The discharge reaction consists of three processes. These are the electron transfer, charge transfer and mass transfer. In this study, we assumed a simplified reaction model, in which the DCR is the summation of *r*, Ret and Rdiff, namely the ohmic resistance, resistance of charge transfer process and mass transfer process, respectively. The theoretical equation of *r*, Ret and Rdiff is derived from the traditional electrochemical equation by applying it to the porous electrode model of the lead–acid battery [7–9]. This theoretical equation is a function of several parameters of the lead–acid battery. The parameters are porosity, $[SO_4^{2-}]$, electrode toughness and SOC. Fig. 6 shows a comparison between the calculated values from the theoretical equation and the measurement values. These values agree with each other, so our model is very proper and we find Ret, that is, the resistance of the charge transfer process, has a very significant effect on the SOC–DCR relationship. This equation helps to inter-

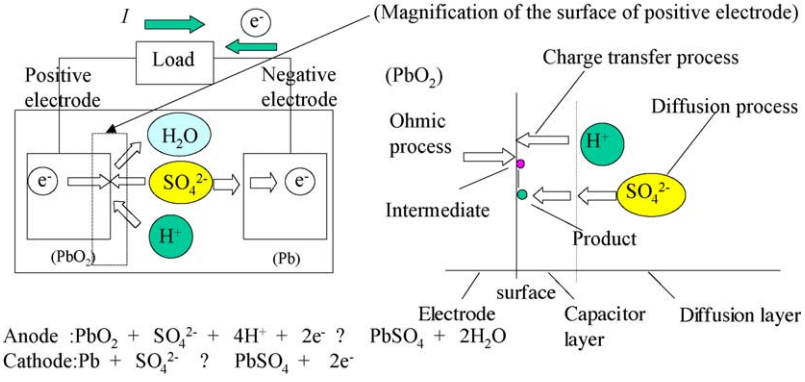

Fig. 5. Reaction process on the surface of the lead–acid battery electrode during discharge.

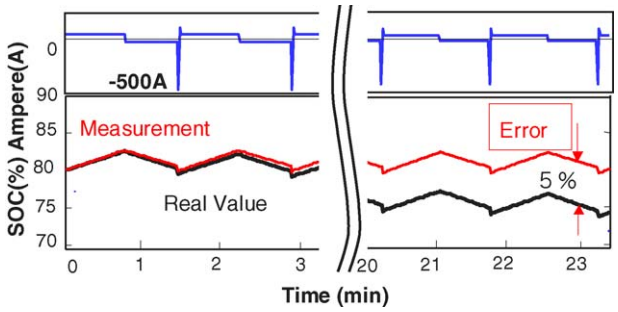

Fig. 7. Method of SOC estimation by current integration method.

polate the data and improve the accuracy of the SOC–DCR table.

3.4. Development of highly accurate SOC measurement method

The SOC measurement schemes are classified into the SOC–DCR table, current integration and a combination of both.

In the current integration method, the SOC is measured by the following equations.

$$\mathrm{SOC} = \mathrm{SOC} + \Delta\mathrm{SOC}(j) \tag{3}$$

$$\Delta\mathrm{SOC}(j) = \int I\,\mathrm{d}t \tag{4}$$

ΔSOC is the value of the integration of current in unit time. In this case, the unit time is one second. ΔSOC is added to the SOC value. Fig. 7 shows the SOC measurement using the current integration method. The full scale of the current sensor is 500 A. The measurement error of the current sensor is 0.1% full scale. The measurement error accumulated with time and after 23 min, the measurement error reached 5%. So this method is not good for utilization when measuring a large current as during engine cranking. We need a highly accurate and expensive current sensor. But advantage of this method is that the measurement error in the short range is low.

On the other hand, in the SOC–DCR method, the SOC is calculated by using the SOC–DCR table. The DCR is measured by Eq. (2). Fig. 8 shows the SOC estimation using the SOC–DCR table method. As shown, the error in the SOC measurement is

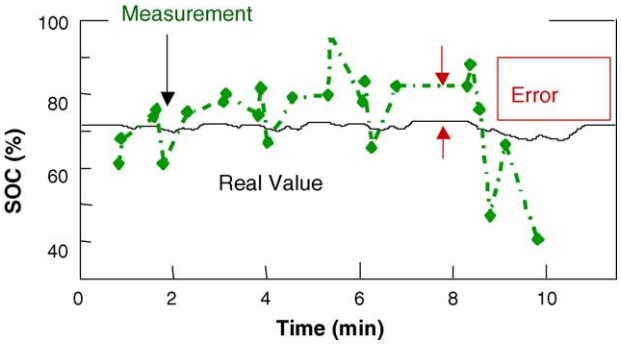

Fig. 8. Subject of SOC estimation by DCR method.

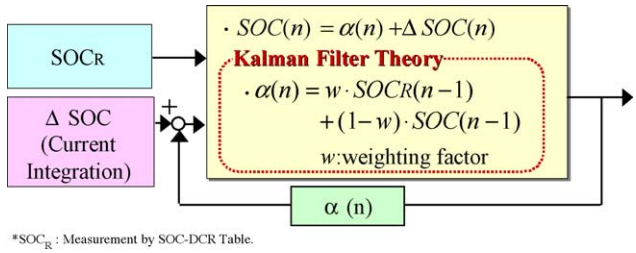

Fig. 9. Algorithm of SOC measurement using Kalman Filter Theory.

large especially in the high SOC region. Because, as previously mentioned, the sensitivity of SOC–DCR relationship is very low in the high SOC region. However, the advantage of this method is that the measurement error does not accumulate with time.

Therefore, we used the combination of both as the SOC measurement. We applied the Kalman Filter Theory [10–12] to the SOC measurement. The advantage of both is combined with using weighting factor.

Fig. 9 shows the algorithm of the SOC measurement using the Kalman Filter Theory. $\alpha(n)$ is the averaged value of $\mathrm{SOC_R}$, that is calculated by the SOC–DCR table and SOC using weighting factor,"w". The weighting factor is determined by considering the measuring error of the $\mathrm{SOC_R}$ and SOC. ΔSOC is measured by current integration versus time. ΔSOC is added to the Kalman Filter result, $\alpha(n)$. The advantage of this method is as follows: first, error of the $\mathrm{SOC_R}$ is decreased by the weighting factor and second, the error of SOC value can be revised at any time.

Fig. 10 shows the evaluation result for the VRLA. The test condition is determined by the case, when the car system is 42 V and loaded with a 4 kW motor generator and has the function of regeneration and power assist. Current is produced by a precise charge and discharge system. The initial SOC has a 30% SOC

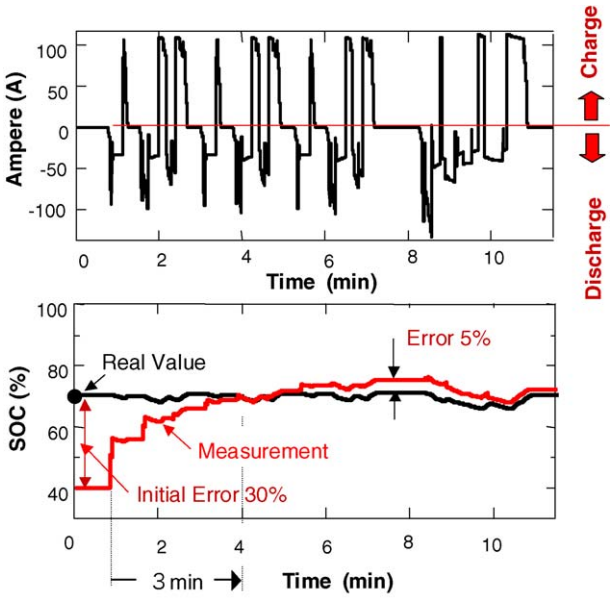

Fig. 10. Evaluation result for VRLA. Temperature: 25 °C; Test sample: VRLA 36 V, 19 Ah (0.2 C). Charge and discharge current: generated by simulation for 4 kW motor generator 42 V system.

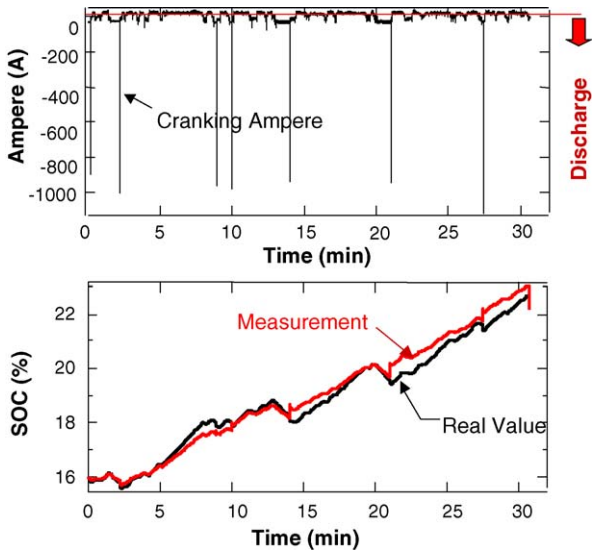

Fig. 11. Evaluation result for the flooded type. Temperature: 25 °C; Test sample: liquid type 12 V, 100 Ah (0.2 C). Charge and discharge current: generated by simulation for the case of ISS 14 V system.

error. The measurement error decreased with time and reached to ±5%. The initial error, 30%, is reduced within 3 min.

Fig. 11 shows the evaluation result for the flooded type. The test condition is when the car has an ISS system and is loaded with an 80 Ah flooded type 12 V lead–acid battery. The current is produced by a precise charge and discharge system. The initial SOC is estimated by the open circuit voltage of the battery. The measurement error is very small.

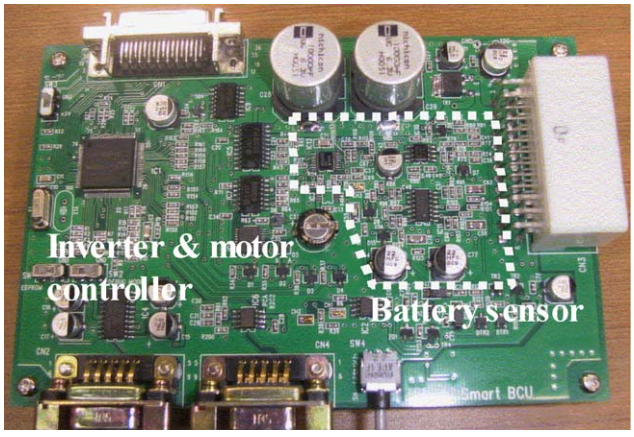

Fig. 12. Sample of battery controller.

3.5. Sample of battery controller

Fig. 12 shows the battery controller. It consists of a battery voltage sensor, current integration IC, shunt, which measures the current, microcontroller and so on. This has the function of communicating with other devices through a LAN cable. This device is shared with the inverter and motor controller. In this white and broken line area there is the battery controller (BC), The SOC is measured in this inverter and motor controller which is also used for the inverter control .The precision of the sensors for the voltage, current, temperature is 0.5% full scale. We expect the cost is reduced by this sharing method.

4. Conclusions

(1) A novel battery condition monitoring (BCM) technology for the lead–acid batteries has been developed.
(2) We select DCR as the SOC measurement parameter.
(3) In order to improve the accuracy of the SOC–DCR table, we have derived a theoretical equation of SOC–DCR relationship.
(4) We developed the original algorithm of measuring the SOC of lead–acid batteries using the Kalman Filter Theory. By using the algorithm, the SOC of a lead–acid battery can be very accurately measured.

References

[1] K. Hata, et al., JARI Res. J. 99 (1999) 13.
[2] T. Teratani, et al., Denki-Kagaku 122 (2002) 356.
[3] T.J. Dougherty, Proposed New Data Parameters for Battery Simulation and Monitoring, MIT Consortium Subcomittee in Plymouth, 2001.
[4] H. Hirotani, et al., Shin-Kobe Tech. Rep. 6 (1995) 19.
[5] K. Champlin, et al., Battery Council Int. (2001).
[6] W.B. Gu, et al., J. Electrochem. Soc. 144 (1997) 2053.
[7] Tanaka, et al., GS News Tech. Rep. 43 (1984) 12.
[8] Yoshida, et al., GS News Tech. Rep. 36 (1977) 98.
[9] W.B. Gu, et al., J. Electrochem. Soc. 144 (1997) 2053.
[10] S. Piller, et al., J. Power Sources 96 (2001) 113.
[11] R. Kalman, Trans. ASME J. Basic Eng. Ser. D 82 (1960).
[12] T. Kinoshita, et al., Denkigakkai-Jidoushakenkyukai, VT-03-7, (2003).